PRECONDITIONING THE JACOBIAN SYSTEM OF THE EXTREME TYPE–II GINZBURG–LANDAU PROBLEM

NICO SCHLÖMER* AND WIM VANROOSE†

Abstract. This present paper considers the extreme type–II Ginzburg–Landau equations that model vortex patterns in superconductors. The nonlinear PDEs are solved using Newton's method where preconditioning the linear solver of the Jacobian system is crucial for the performance of the algorithm. Some of the properties of the Jacobian operator will be highlighted, emphasizing on how a multilevel approach is crucial with the construction of an optimal preconditioner.

Key words. Ginzburg–Landau equations, nonlinear problems, preconditioning, multigrid, numerical computation

1. Introduction. The nonlinear Schrödinger equation is used in many areas of science and technology and describes, for example, the propagation of solutions in fiber optics or Bose-Einstein condensates in ultra cold traps. The Ginzburg–Landau equations is a prototype of such an equation that is used to model the state and the magnetic field inside superconducting nanodevices. To understand the dynamics of these systems, it is critical to have an efficient solver such that the solution space of can be efficiently explored by, for example, numerical continuation.

In this paper, we describe a multigrid-preconditioned Krylov solver for the Ginzburg–Landau equations. In section 2, we describe the equations in question and section 3 discusses properties of the linearization with respect to numerical algorithms. While section 4 briefly introduces the applied discretization, section 5 contains the proposed algorithm and considers a multigrid strategy. The documents concludes with a discussion of the performance of the solver.

2. The Ginzburg–Landau equations. For an open, bounded domain $\Omega \subseteq \mathbb{R}^n$ with a piecewise smooth boundary $\partial\Omega$, the celebrated Ginzburg–Landau problem is usually stated as a minimization problem of the Gibbs free energy functional. Using standard calculus of variations, this leads to the much acclaimed Ginzburg–Landau equations

$$\begin{cases} 0 = \left(-\mathbb{i}\boldsymbol{\nabla} - \mathbf{A}\right)^2 \psi - \psi\left(1 - |\psi|^2\right) & \text{on } \Omega \\ \mathbf{0} = -\kappa\boldsymbol{\nabla} \times (\boldsymbol{\nabla} \times \mathbf{A}) - \Im(\overline{\psi}\boldsymbol{\nabla}\psi) + |\psi|^2\mathbf{A} & \text{on } \Omega \cup \partial\Omega \\ \mathbf{0} = -\kappa\boldsymbol{\nabla} \times (\boldsymbol{\nabla} \times \mathbf{A}) & \text{on } \mathbb{R}^n \backslash (\Omega \cup \partial\Omega) \\ \mathbf{n} \cdot (-\mathbb{i}\boldsymbol{\nabla} - \mathbf{A})\psi|_\Gamma = 0 \\ \lim\limits_{\|x\| \to \infty} \boldsymbol{\nabla} \times \mathbf{A} = \mathbf{H}_0 \end{cases} \tag{2.1}$$

over $\psi \in H^2_{\mathbb{C}}(\Omega)$ and $\mathbf{A} \in H^2_{\mathbb{R}^n}(\Omega)$. ψ is commonly referred to as *order parameter*; $\mathbf{A}$ is the magnetic vector potential corresponding to the induced magnetic field. The outward unit surface normal on $\partial\Omega$ is denoted by $\mathbf{n}$. Parameters to the systems

*Departement Wiskunde-Informatica, Universiteit Antwerpen, Middelheimlaan 1, 2020 Antwerpen, Belgium

†Departement Wiskunde-Informatica, Universiteit Antwerpen, Middelheimlaan 1, 2020 Antwerpen, Belgium

are the given external magnetic field $\mathbf{H}_0$; the parameter $\kappa = \lambda/\xi$ is related to the coherence length ξ, the characteristic length of change in the order parameter ψ, and the penetration depth λ, a length scale on which the magnetic field penetrates the sample. For $\kappa < 1/\sqrt{2}$, the superconductor is said to be of type I, and of type II otherwise. In the present paper, the domain Ω is scaled in units of the coherence length ξ.

The physical observables are the Cooper pair density $\rho_C = |\psi|^2$ and the induced magnetic field $\mathbf{B} = \boldsymbol{\nabla} \times \mathbf{A}$.

The trivial solution, $\psi = 0$, is the normal non-superconducting state which is the lowest energy state for fields above the critical magnetic field strength. For weak magnetic fields, however, there are non-zero solutions that have a lower energy. These are the famous vortex solutions where the magnetic field penetrates the sample (see figure 2.1).

It is immediately obvious that the numerical difficulties in solving (2.1) include the fact that the domain of $\mathbf{A}$ is infinitely large, $\mathbb{R}^n$. Significant fluctuations in $\mathbf{A}$ will indeed damp out further away from the sample, such that the boundary conditions on $\mathbf{A}$ can sensibly be demanded on the boundary of a finite domain $\Omega_2 \supset \Omega$, but it is not possible to determine a priori how large Ω_2 needs to be to capture the physical effects.

2.1. Extreme type–II case. Extreme type–II superconductors occur, for example, in the field of high-temperature superconductors; they are all of type II and typically $50 \ll \kappa$.

For $\kappa \to \infty$, the equations (2.1) decouple and $\mathbf{A} = \mathbf{A}(\mathbf{H}_0)$ is given by the relations

$$\begin{cases} \boldsymbol{\nabla} \times (\boldsymbol{\nabla} \times \mathbf{A}) = 0, \\ \lim\limits_{\|x\| \to \infty} \boldsymbol{\nabla} \times \mathbf{A} = \mathbf{H}_0. \end{cases}$$

To rigorously formulate the governing equation for ψ, let us introduce

$$\begin{aligned} X := \big\{ \psi \in H^2(\Omega) : &\text{ there is a defining sequence } \psi_k \text{ with} \\ &\lim\nolimits_{k\to\infty} \mathbf{n} \cdot (-\mathbb{i}\boldsymbol{\nabla} - \mathbf{A}(\mu))\psi_k = 0 \text{ on } \partial\Omega \big\}, \\ Y := L^2(\Omega). & \end{aligned}$$

We shall look for (weak) solutions $\psi \in X$ of

$$\begin{aligned} \mathcal{GL}(\psi) &: X \to Y \\ 0 = \mathcal{GL}(\psi) &:= \left(-\mathbb{i}\boldsymbol{\nabla} - \mathbf{A}\right)^2 \psi - \psi \left(1 - |\psi|^2\right) \quad \text{on } \Omega \end{aligned} \tag{2.2}$$

Note that, for convex Ω and $\mathbf{A} \in C^\infty(\overline{\Omega})$, such solutions immediately have higher regularity [1] and in fact coincide with the classical strong solutions in $C^2(\Omega) \cap C^1(\overline{\Omega})$.

3. Newton's method and properties of the Jacobian operator. In this section, properties of the (continuous) Jacobian operator will be elaborated on. Some of the retrieved results will also be of use for the later construction of preconditioners and will be referred to in section 5. While the following results all translate into the discrete space when changing the respective domains and ranges accordingly, details on this will not be worked out here.

Equation (2.2) is a nonlinear equation in ψ and hence classically suited for treatment with Newton's method. While there were efforts in solving (2.2) with a modified algorithm [5], the generic approach of the full Newton system is applied here

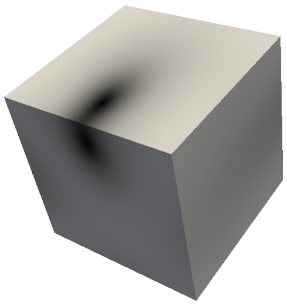

(a) Solution for a rather low applied magnetic field on a solid $10 \times 10 \times 10$ cube. 1.0×10^6 complex-valued unknowns.

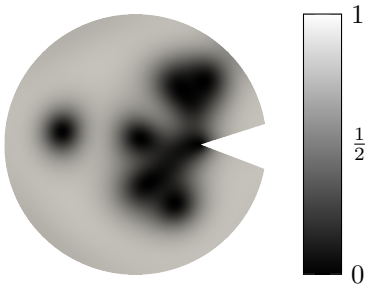

(b) Solution for a higher magnetic field on a "Pac-Man" domain. Approx. 1.5×10^5 complex-valued unknowns.

Fig. 2.1: Typical solutions $|\psi|^2$ of the Ginzburg–Landau equations for different domains. Amongst the recurring features are especially the vortex structures which become more involved as the applied magnetic field is increased.

for its attractive second order convergence. First, the equations for the Newton update $\delta\psi$ at $\psi \in Y$ are formulated in the continuous framework, i.e.,

$$\mathcal{J}(\psi)\delta\psi = -\mathcal{GL}(\psi), \tag{3.1}$$

and subsequently discretized [7].

To retrieve a representation of the Jacobian operator, consider for given Ω, $\mathbf{H}_0$, and $\psi, \delta\psi \in X$

$$\begin{aligned}
&\mathcal{GL}(\psi + \delta\psi) - \mathcal{GL}(\psi) \\
&= \left[(-\mathbb{i}\boldsymbol{\nabla} - \mathbf{A})^2(\psi + \delta\psi) - (\psi + \delta\psi)\left(1 - \overline{(\psi + \delta\psi)}(\psi + \delta\psi)\right)\right] \\
&\quad - \left[(-\mathbb{i}\boldsymbol{\nabla} - \mathbf{A})^2\psi - \psi\left(1 - \overline{\psi}\psi\right)\right] \\
&= (-\mathbb{i}\boldsymbol{\nabla} - \mathbf{A})^2\delta\psi + \psi\left(\overline{\psi}\,\delta\psi + \psi\,\overline{\delta\psi} + \overline{\delta\psi}\,\delta\psi\right) \\
&\qquad\qquad - \delta\psi\left(1 - \overline{\psi}\psi\right) \\
&\qquad\qquad + \delta\psi\left(\overline{\psi}\,\delta\psi + \psi\,\overline{\delta\psi} + \overline{\delta\psi}\,\delta\psi\right).
\end{aligned}$$

Neglecting the second- and higher order terms in $\delta\psi$, this yields the Jacobian operator

$$\begin{aligned}
&\mathcal{J}(\psi) : X \to Y, \\
&\mathcal{J}(\psi)\varphi := \left((-\mathbb{i}\boldsymbol{\nabla} - \mathbf{A})^2 - 1 + 2|\psi|^2\right)\varphi + \psi^2\overline{\varphi}.
\end{aligned} \tag{3.2}$$

Note that $\mathcal{J}(\psi)$ is indeed linear for all ψ when defined over X and Y as $\mathbb{R}$-vector spaces.

The kinetic energy operator. Before analyzing the Jacobian operator $\mathcal{J}(\psi)$ as a whole, we will take a close look at the part that is commonly referred to as the *kinetic energy operator*,

$$\begin{aligned}
&\mathcal{K}\colon X \to Y, \\
&\mathcal{K}\varphi := (-\mathbb{i}\boldsymbol{\nabla} - \mathbf{A})^2\varphi.
\end{aligned} \tag{3.3}$$

This operator is (classically) linear, and has several other properties that will be useful later on.

Firstly, by subsequent application of Green's first identity, it is easy to prove

LEMMA 3.1. *Let $\mathbf{A} \in C^1_{\mathbb{R}^d}(\Omega)$. The kinetic energy operator (3.3) is self-adjoint with respect to the inner product $\langle \cdot, \cdot \rangle_{L^2(\Omega)}$.*

Proof. See [8]. □

This means nothing else than that all eigenvalues of $\mathcal{K}$ are real valued. However, even more can be stated about its spectrum. Consider

LEMMA 3.2. *Let $\mathbf{A} \in C^1_{\mathbb{R}^d}(\Omega)$. Then*

$$\int_\Omega \overline{\psi}(-\mathbb{i}\boldsymbol{\nabla} - \mathbf{A})^2 \varphi \, \mathrm{d}\Omega = \int_\Omega \overline{(-\mathbb{i}\boldsymbol{\nabla} - \mathbf{A})\psi}(-\mathbb{i}\boldsymbol{\nabla} - \mathbf{A})\varphi \, \mathrm{d}\Omega$$

for all $\psi \in L^2_{\mathbb{C}}(\Omega)$, $\varphi \in X$.

Proof. See [8]. □

It follows that the kinetic energy operator is positive semidefinite in the $L^2(\Omega)$ inner product: For all $\psi \in X$, it is, by lemma 3.2,

$$\langle \psi, \mathcal{K}\psi \rangle_{L^2\Omega} = \int_\Omega \overline{\psi}\widehat{L}\psi \, \mathrm{d}\Omega = \int_\Omega \left\| (-\mathbb{i}\boldsymbol{\nabla} - \mathbf{A})\psi \right\|^2 \mathrm{d}\Omega \geq 0.$$

Moreover, the value of 0 is attained if and only if

$$(-\mathbb{i}\boldsymbol{\nabla} - \mathbf{A})\psi = 0 \text{ a.e. on } \Omega,$$

from which in turn follows that

$$\begin{aligned} 0 = \boldsymbol{\nabla} \times (-\mathbb{i}\boldsymbol{\nabla}\psi) - \boldsymbol{\nabla} \times (\mathbf{A}\psi) &= -\mathbb{i}(\boldsymbol{\nabla} \times \boldsymbol{\nabla}\psi) - (\boldsymbol{\nabla} \times \mathbf{A})\psi - (\boldsymbol{\nabla}\psi) \times \mathbf{A} \\ &= -\mathbf{H}_0\psi - \mathbb{i}\mathbf{A} \times \mathbf{A} = -\mathbf{H}_0\psi \text{ a.e. on } \Omega. \end{aligned} \quad (3.4)$$

Hence, only for vanishing magnetic fields $\mathbf{H}_0$, the kinetic energy operator $\mathcal{K}$ is actually degenerate.

These results give a lot more structure to the Jacobian operator $\mathcal{J}(\psi)$ already: For any given $\psi \in X$, $\mathcal{J}(\psi)$ is the composition of a self-adjoint, positive (semi)definite operator and some reaction terms. It should be possible to infer certain properties on $\mathcal{J}$ starting from here. From a numerical point of view, insight into the adjointness and the spectrum of the operator will be highly desirable.

The peculiar structure of $\mathcal{J}(\psi)$, acting on φ and its pointwise conjugate adjoint, though, make it necessary to look at inner products other than the regular $\langle \cdot, \cdot \rangle_{L^2(\Omega)}$. The following lemma sheds light onto what the adjoint of a linear operator of the form (3.2) looks like. For the sake of generality, it is formulated for general Hilbert spaces, and in our specific case $H = L^2_{\mathbb{C}}(\Omega)$, the operation θ will be the pointwise complex conjugation.

LEMMA 3.3. *Let H be a Hilbert-space with inner product $\langle \cdot, \cdot \rangle_H$ and let there be an operation $\theta : H \to H$ such that*

$$\begin{aligned} \theta(\alpha x) &= \alpha\theta(x), \quad \alpha \in \mathbb{R} \\ \Re \langle \theta(x), y \rangle_H &= \Re \langle x, \theta(y) \rangle_H \end{aligned} \quad (3.5)$$

for all $x, y \in H$. Let $\mathcal{L}_1, \mathcal{L}_2 : H \to H$ be linear operators. For every $x \in H$, let

$$\mathcal{L}x := \mathcal{L}_1 x + \mathcal{L}_2 \theta(x).$$

Then $\mathcal{L}$ is linear as operator on H as $\mathbb{R}$-vector space, and its adjoint $\mathcal{L}^*$ with respect to the inner product $\langle\cdot,\cdot\rangle_{\mathbb{R}} := \Re\langle\cdot,\cdot\rangle_H$ is given by

$$\mathcal{L}^* x := \mathcal{L}_1^* x + \theta(\mathcal{L}_2^* x),$$

where $\mathcal{L}_1^*$, $\mathcal{L}_2^*$ are the adjoint operators of $\mathcal{L}_1$, $\mathcal{L}_2$, respectively, with respect to $\langle\cdot,\cdot\rangle_H$.

Proof. See [8]. □

With the help of lemma 3.1, it can now easily be concluded that

COROLLARY 3.4. *For any given $\psi \in Y$, the Jacobian operator $\mathcal{J}(\psi)$ (3.2) is linear and self-adjoint with respect to the inner product*

$$\langle\cdot,\cdot\rangle_{\mathbb{R}} := \Re\langle\cdot,\cdot\rangle_{L^2(\Omega)}. \tag{3.6}$$

REMARK 1. *Note that $\langle\cdot,\cdot\rangle_{\mathbb{R}}$ coincides with the natural inner product in $(\mathcal{L}^2_{\mathbb{R}}(\Omega))^2$ which is isomorphic to $L^2_{\mathbb{C}}(\Omega)$, as for any given pair $\phi,\psi \in L^2_{\mathbb{C}}(\Omega)$ it is*

$$\left\langle \begin{pmatrix}\Re\phi\\ \Im\phi\end{pmatrix}, \begin{pmatrix}\Re\psi\\ \Im\psi\end{pmatrix} \right\rangle_{(L^2_{\mathbb{R}}(\Omega))^2} = \langle\Re\phi,\Re\psi\rangle_{L^2_{\mathbb{R}}(\Omega)} + \langle\Im\phi,\Im\psi\rangle_{L^2_{\mathbb{R}}(\Omega)} = \langle\phi,\psi\rangle_{\mathbb{R}}.$$

This can be relevant in practice as quite commonly, the complex-valued original problem (2.2) in $L^2_{\mathbb{C}}(\Omega)$ is implemented in terms $(\mathcal{L}^2_{\mathbb{R}}(\Omega))^2$. Using the natural inner product in this space (wherever an algorithm uses it, e.g., CG*) will yield the expected results without having to take particular care of $\Re\langle\cdot,\cdot\rangle_{L^2(\Omega)}$.*

Now that the spectrum of $J(\psi)$ is known to be a subset of $\mathbb{R}$ as well, the next natural question to ask is whether or not $J(\psi)$ is generally definite. Unfortunately, no such thing is true. Quite the contrary: Note that for a solution ψ_{s} of (2.2), it is

$$\begin{aligned}\mathcal{J}(\psi_{\mathrm{s}})(\mathrm{i}\psi_{\mathrm{s}}) &= \left[(-\mathrm{i}\boldsymbol{\nabla} - \mathbf{A})^2 - 1 + 2|\psi_{\mathrm{s}}|^2\right](\mathrm{i}\psi_{\mathrm{s}}) - \mathrm{i}\psi_{\mathrm{s}}^2\overline{\psi_{\mathrm{s}}} \\ &= \left(1 - |\psi_{\mathrm{s}}|^2\right)(\mathrm{i}\psi_{\mathrm{s}}) - \mathrm{i}\psi_{\mathrm{s}} + 2\mathrm{i}\overline{\psi_{\mathrm{s}}}\psi_{\mathrm{s}}^2 - \mathrm{i}\psi_{\mathrm{s}}^2\overline{\psi_{\mathrm{s}}} = 0, \end{aligned} \tag{3.7}$$

and hence $\operatorname{span}\{\mathrm{i}\psi_{\mathrm{s}}\} \subseteq \ker\mathcal{J}(\psi_{\mathrm{s}})$. This is a direct consequence of the fact that (2.2) is invariant under the gauge transformation $\widetilde{\psi} = \exp(\mathrm{i}\chi)\psi$ for any $\chi \in \mathbb{R}$. One serious implication of (3.7) is that the nullspace of the Jacobian operator in a solution ψ_{s} is unconditionally nontrivial if $\psi_{\mathrm{s}} \neq 0$.

Besides the fact that there is always a degenerate eigenvalue and that all eigenvalues are real, not much more can be said about the spectrum; in general, $\mathcal{J}(\psi)$ is indefinite. The definiteness depends entirely on the state ψ; if ψ is a solution to (2.2), it is said to be stable or unstable depending whether or not $\mathcal{J}(\psi)$ has positive eigenvalues. Typically, solutions with low energies (relative to the applied magnetic field) tend to be stable whereas solutions with high energies tend to be unstable. However, it is uncommon to see more than ten negative eigenvalues for a given solution state.

4. Link variables and discretization in finite volumes. Naive discretization schemes of the Ginzburg–Landau equations (2.2) lead to a system which preserves gauge invariance, inherent to the Ginzburg–Landau equations, only up to a certain order. Thus, it is customary to reformulate (2.2) in such a way that gauge invariance is preserved exactly in pointwise discretizations. For any given normalized spatial direction $\mathbf{v}$, let

$$U_{\mathbf{v}}(\mathbf{x}) := \exp\left(-\mathrm{i}\int_{\hat{\mathbf{x}}}^{\mathbf{x}} \mathbf{v}\cdot\mathbf{A}(\mathbf{w})\,\mathrm{d}\mathbf{w}\right),$$

with arbitrary, fixed $\hat{\mathbf{x}} \in \mathbf{x} + \operatorname{span}\{\mathbf{v}\}$ (e.g., $\hat{\mathbf{x}} = \mathbf{x} - (\mathbf{x}\cdot\mathbf{v})\mathbf{v}$). With this, one has

$$-\mathbb{i}\overline{U}_{\mathbf{v}}\mathbf{v}\cdot\boldsymbol{\nabla}(U_{\mathbf{v}}\psi) = -\mathbb{i}\overline{U}_{\mathbf{v}}\left(-\mathbb{i}\mathbf{v}\cdot\mathbf{A}U_{\mathbf{v}}\psi + U_{\mathbf{v}}\mathbf{v}\cdot\boldsymbol{\nabla}\psi\right) = \mathbf{v}\cdot(-\mathbb{i}\boldsymbol{\nabla} - \mathbf{A})\psi.$$

Upon integrating the Ginzburg–Landau equations (2.2) over a control volume Ω_k, one gets

$$\begin{aligned} 0 = \int_{\Omega_k} \left(-\mathbb{i}\boldsymbol{\nabla} - \mathbf{A}\right)^2 \psi - \psi\left(1 - |\psi|^2\right) &= \int_{\partial\Omega_k} \mathbf{n}\cdot\left(-\mathbb{i}\boldsymbol{\nabla} - \mathbf{A}\right)\psi - \int_{\Omega_k} \psi\left(1-|\psi|^2\right) \\ &= \int_{\partial\Omega_k} -\mathbb{i}\overline{U}_{\mathbf{n}}\mathbf{n}\cdot\boldsymbol{\nabla}(U_{\mathbf{n}}\psi) - \int_{\Omega_k}\psi\left(1-|\psi|^2\right) \quad (4.1) \end{aligned}$$

If the finite volumes Ω_k are canonically constructed of a triangulation of the domain, then the edges of the triangulation coincide with the outer normals $\mathbf{n}$ of the finite volumes. The boundaries of all Ω_k are piecewise linear and its pieces P are perpendicular to the edges of the triangulation. For two-dimensional domains, P is often referred to as the *co-edge*; in three dimensions P generally is a two-dimensional polyhedron. The integral over each piece is then simply approximated by a one-point-rule. This yields

$$\int_{\partial\Omega_k} -\mathbb{i}\overline{U}_{\mathbf{n}}\mathbf{n}\cdot\boldsymbol{\nabla}(U_{\mathbf{n}}\psi) \approx \sum_{\text{pieces } P \text{ of } \partial\Omega_k} -\mathbb{i}|P|\frac{\widetilde{U}\psi_{k,P} - \psi_k}{\|\mathbf{x}_{k,P} - \mathbf{x}_k\|}$$

where

$$\widetilde{U} := \exp\left(-\mathbb{i}\int_{\mathbf{x}_k}^{\mathbf{x}_{k,P}} \frac{\mathbf{x}_{k,P} - \mathbf{x}_k}{\|\mathbf{x}_{k,P} - \mathbf{x}_k\|}\cdot\mathbf{A}(\mathbf{w})\,\mathrm{d}\mathbf{w}\right),$$

and ψ_k, $\psi_{k,P}$ are the function value at the two sides of P. Approximating the latter by

$$\widetilde{U} \approx \widetilde{U}_h := \exp\left(-\mathbb{i}(\mathbf{x}_{k,P} - \mathbf{x}_k)\cdot\mathbf{A}\left(\tfrac{\mathbf{x}_{k,P}+\mathbf{x}_k}{2}\right)\right)$$

and approximating the nonlinear term in (4.1) by mass lumping, one eventually arrives at the discretization

$$0 = \sum_{\text{pieces } P \text{ of } \partial\Omega_k} -\mathbb{i}|P|\frac{\widetilde{U}_h\psi_{k,P} - \psi_k}{\|\mathbf{x}_{k,P} - \mathbf{x}_k\|} - |\Omega_k|\psi_k\left(1 - |\psi_k|^2\right) \quad (4.2)$$

for each control volume with unknowns ψ_k. All P and $\mathbf{x}_k$ are given by the triangulation, $\widetilde{U}_h$ is given by the magnetic vector potential.

This formulation has several advantages, starting with the fact that the boundary conditions of the Ginzburg–Landau equations (2.2) are naturally contained in the discretization. Also, the first expression in (4.2) exactly coincides, up to the terms $\widetilde{U}_h$, with the canonical finite volume discretization of the Laplace operator. This makes the discretization readily implementable, and the sparsity structure of the corresponding matrices will not be unpleasantly dense.

Moreover – and this will not be shown in detail here – the Jacobian operator of the discretized problem (4.2) inherits all the properties of the continuous Jacobian of the the corresponding problem in section 3. Particularly, the discrete Jacobian operator is self-adjoint in the discretized scalar product $\mathbb{R}\langle\cdot,\cdot\rangle_{\ell^2(\Omega_h)}$, and the discretized kinetic energy operator is self-adjoint and positive (semi)definite.

5. Algorithm and numerical results. To solve the discretized system (4.2), Newton's method will be the method of choice for its second order convergence. The systems with the Jacobian matrix that will need to be solved in each step can be approached with symmetric methods as the problem is self-adjoint (see corollary 3.4). However, note that the specific implementation has to take into account the inner product (3.6).

As the definiteness of $\mathcal{J}(\psi)$ highly depends on current guess for ψ and as it is in any case degenerate, MINRES appears most suitable choice from the classical symmetric algorithms. Also CG is known to perform well for indefinite problems if the number of negative eigenvalues is not too large, the convergence, however, can be irregular.

5.1. Preconditioning. As the main computational effort of the nonlinear solver will flow into the linear solves of the Jacobian system, the immediate question is how to speed up the Krylov iteration with a preconditioner. Given the results of section 3, the kinetic energy operator K attracts attention: Not only is it structurally closely related to the Jacobian, it also has a number of convenient properties, such as

- K is a linear operator in the classical sense;
- K is classically self-adjoint and positive (semi)definite.

These make it possible to solve system with K in numerous ways and hence it appears to be a good candidate for a preconditioner. Tests for small systems which permit exact (LU) inversion of K then indeed show (see figure 5.1) that it ensures a constant number of iterations of the outer (CG or MINRES) iteration *independent of the number of unknowns*. This is indeed all that can be expected.

It is now crucial to find out about how systems with K can be solved in a quick, memory-efficient, and scalable manner. This is where multigrid methods are indispensable: The operator K to be inverted is Hermitian, positive definite, derived from a geometric discretization, and its sparsity structure coincides with that of the Laplacian with purely Neumann boundary conditions. In fact, the magnitudes of the entries are exactly the same. The only mild difficulty – when applying algebraic multigrid methods – stems from the fact that matrix entries are complex-valued. Difficulties in this area however have already been treated [6]. Based on the results in [6], it is to be expected that linear systems with K, when approached with an (A)MG-preconditioned CG solver, can be solved with a number of iterations that is independent of the number of unknowns.

Computational experiments have been conducted for two representative domains (cf. figure 2.1) and various magnetic vector potentials. See figure 5.2 for results.

Scalability. A crucial aspect for computational needs of the scale that is presented in this paper is the question of the scalability of the algorithm. It is most often not anymore feasible to perform the computations on a limited number of cores, particularly in light of the current trend in hardware development towards many-core architectures. Hence, it is important to identify possible bottlenecks in the parallelizability of a given algorithm.

For the present case, the computationally most intensive parts will be matrix-vector products and the multigrid solves. The former, however, are trivially parallelized if one carefully distributes the rows of respective matrices as well as the given vectors. There is also extensive theory for parallel implementations of (algebraic) multigrid solvers. In the present paper, the advantages of the ML package [4] are leveraged together with its Trilinos framework [3]. For computational results, see figure 5.3.

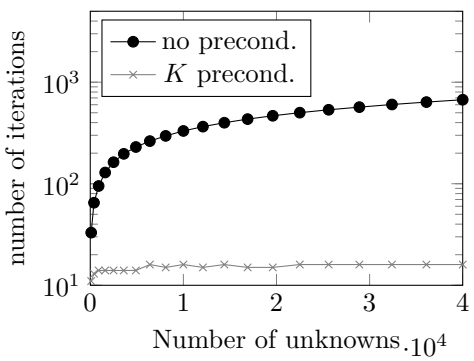

(a) Linear solver applied to test problems for different mesh sizes. In all cases, the initial guess chosen as $x_0 = 0$, the right hand side $b = 1 + \mathrm{i}$. The magnetic vector potential was chosen rather small, i.e., $\|\mathbf{A}\| \approx 0.01$ throughout the domain.

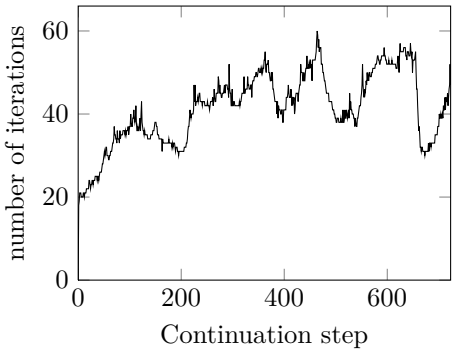

(b) The number of iterations of the linear solver for a series of different ψ and $\mathbf{A}$, taken of a numerical continuation run with μ as parameter. The number of unknowns is constant throughout the computation ($\approx 3 \times 10^5$), but ψ and hence the spectrum of $\mathcal{J}(\psi)$ changes in every step.

Fig. 5.1: Convergence of MINRES applied to $J(\psi)$ with the kinetic energy operator as preconditioner (solved with LU) in different contexts. The grid was in all cases a discretization of the two-dimensional domain as displayed in figure 2.1b. ψ was chosen to be $0.5 + \mathrm{i}0.5$ with random fluctuation of magnitude at most 0.1. The magnetic vector potential was chosen to be $\mathbf{A} = (-\mu y, \mu x, 0)$ with $\mu = 0.1$. This corresponds to a magnetic field applied in z-direction. The iterations were aborted as soon as $\|r\| < 10^{-10}$ was reached. Note that (a) the preconditioner yields a (nearly) constant number of unknowns if the state remains the same and the number of grid points is increased. (b) On the other and, for a constant number of unknowns and different states as occurring in a continuation run, the number of iterations remains bounded as well.

6. Discussion and conclusions. The authors propose an algorithm for the solution of the extreme type–II Ginzburg–Landau equation that at its heart uses a multigrid strategy which is crucial for the performance and scalability of the algorithm as a whole. Numerical results for two representative domains point towards the optimality of the algorithm in the sense of independence of the number of performed linear solver iterations from the actual problem size. This suggests that, qualitatively, no further improvement can be reached.

The numerical experiments show promising scalability data for 8 cores and less, and the subsequent loss of efficiency can be explained by the particular hardware setup. While, given the building blocks of the algorithm, high efficiency even for a large number of processes is expected, this suggestion will need to stand verification in larger HPC environments.

This research opens up new possibilities for the exploration of the energy landscape of type–II superconductors. Solution of three-dimensional problems is now accessible with grid resolutions on par with current two-dimensional calculations.

To firmly establish the kinetic energy operator as a valid preconditioner for the Jacobian operator, rigorous statements about the spectrum of $\mathcal{K}^{-1}\mathcal{J}$ and particularly its discrete counterpart will need to be made. This part of the future work of the

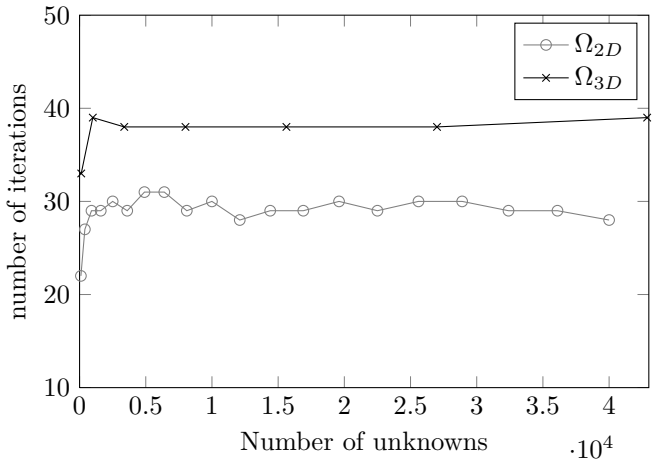

Fig. 5.2: Solving linear problems with K using CG, preconditioned with Chebyshev smoothed aggregation AMG using Trilinos' ML package. The domains in question are FVM discretizations based on (a) a MeshPy-generated triangulation of the "Pac-Man"-shaped domain (see figure 2.1b), and (b) the canonical tetrahedrization of the cube (as shown in figure 2.1a). The applied magnetic field for the displayed results was chosen as in figure 5.1. The critical stopping criterion was chosen to be $\|r\| < 10^{-10}$ in all cases. The experiment clearly displays that the number of iterations is for both domains independent of the actual size of the problem. The experiment has been repeated with several different $\mathbf{A}$ of several magnitudes, and results were always comparable.

authors.

In the multigrid world, a possible alternative for the solution of the nonlinear Ginzburg–Landau equations might be the Full Approximation Scheme (FAS) [2]. However, solvers of this kind have not been approached in the present research. One reason for this is the fact that in practice, the equations are solved in the framework of numerical continuation. Common algorithms there give rise to bordered systems for which Newton's method is indeed the method of choice. However, it may be that the FAS is an efficient stand-alone solver for the Ginzburg-Landau equations.

A natural extension of the presented work is to approach the solution of the full Ginzburg–Landau problem in which the magnetic vector potential cannot be treated as given (2.1). Numerous numerical and computational challenges are posed there. One of the most obvious – restricting the the domain of $\mathbf{A}$ – has received some attention in the past, but no rigorous analysis has been carried out to date.

Acknowledgements. We acknowledge fruitful discussions with Andrew G. Salinger, Gregory D. Sjaardema, and Mark Hoemmen of the Sandia National Laboratories. We are also grateful to the Research Foundation Flanders (FWO) for financial support through the project G017408N.

REFERENCES

[1] C. Bacuta, J.H. Bramble, and J. Xu. Regularity estimates for elliptic boundary value problems

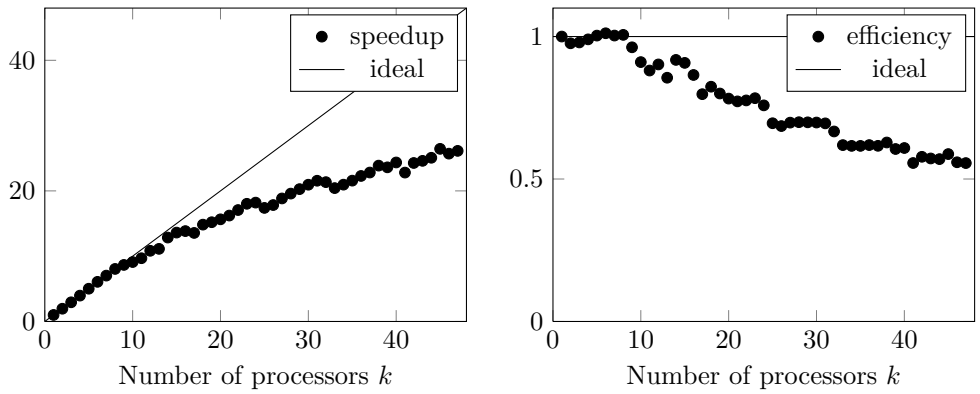

(a) Strong scaling, $s = T_1/T_k$.

(b) Parallel efficiency, s/k.

Fig. 5.3: Scalability test for a full Newton run on the two-dimensional test problem as in figure 2.1b. Measurements have been conducted for other situations, particularly three-dimensional problems, and the results show the same characteristics. All tests have been conducted on a 4-CPU shared-memory machine with AMD Opteron$^{\text{TM}}$ 6174 Processors (12 cores per CPU). Three Newton steps were performed with about 30 linear preconditioned linear iterations for each of the Jacobian solves. The nonlinear solver history (residuals, number of steps) was virtually independent of the number of processors (up to about 10^{-9} in the residuals), so the same number of arithmetic operations was performed. The algorithm scales almost perfectly up to 8 cores, then the efficiency drops to about 0.9 if less then 17 cores are used, at which point there is another drop. This 8-core staircase pattern repeats. This phenomenon has no algorithmic reasons, but is linked to the fact that for memory-CPU communication, the present hardware setup provides two channels per CPU. Two cores per CPU can be provided with data sufficiently fast, but when two cores need to share the bandwidth of one channel (which happens when 9 or more cores are used), this has a serious performance impact. It is expected that the efficiency will be improved on HPCs with a larger memory bandwidth.

with smooth data on polygonal domains. *Journal of Numerical Mathematics*, 11(2):75–94, June 2003.

[2] William L. Briggs, Van E. Henson, and Steve F. McCormick. *A Multigrid Tutorial*. SIAM, 2000.

[3] Michael Heroux et al. An Overview of Trilinos. Technical Report SAND2003-2927, Sandia National Laboratories, 2003.

[4] M.W. Gee, C.M. Siefert, J.J. Hu, R.S. Tuminaro, and M.G. Sala. ML 5.0 smoothed aggregation user's guide. Technical Report SAND2006-2649, Sandia National Laboratories, 2006.

[5] H.G. Kaper and M.K. Kwong. Vortex configurations in type-II superconducting films. *Journal of Computational Physics*, 119(1):120–131, June 1995.

[6] Scott P. MacLachlan and Cornelis W. Oosterlee. Algebraic multigrid solvers for complex-valued matrices. *SIAM Journal on Scientific Computing*, 30(3):1548–1571, 2008.

[7] James M. Ortega and Werner C. Rheinboldt. On discretization and differentiation of operators with application to Newton's method. *SIAM Journal on Numerical Analysis*, 3(1):143–156, 1966.

[8] Nico Schlömer, Daniele Avitabile, and Wim Vanroose. Numerical bifurcation study of superconducting patterns on a square. *Submitted to SIAM Journal on Applied Dynamical Systems*, 2011.